Effect of Cl_2 additions to an argon glow discharge

Nancy L. Bassett and Demetre J. Economou[a)]
Department of Chemical Engineering, Plasma Processing Laboratory, University of Houston, Houston, Texas 77204-4792

(Received 12 July 1993; accepted for publication 5 November 1993)

A steady-state model has been developed to predict the important species densities and the self-sustaining electric field in a plasma. The effect of excited states and radical species produced in the plasma was taken into account in a self-consistent manner. The model was used to study the effect of attaching gas (Cl_2) additions to a noble gas (argon) glow discharge. Specifically a 5% Cl_2/95% Ar discharge was compared to a pristine argon discharge. There are dramatic differences between the two discharges. Most notably, the argon metastable density and the electron density are an order of magnitude lower, while the self-sustaining electric field is much higher for the mixture. The electron density increased with pressure in pure argon, but the inverse trend was predicted for the mixture. Results from this work are compared to available experimental data where possible, and reasonable agreement is obtained.

I. INTRODUCTION

Mixtures of reactive with rare gases are often used for thin film etching and deposition in microelectronic device fabrication. For example, Cl_2/Ar mixtures are common for etching polysilicon. Several studies have been conducted to determine the effect of adding attaching gases to rare gas plasmas.[1–3] However, the plasma chemistry of gas mixtures is poorly understood. For example, how is the electron energy distribution function being affected, and what is the role of metastables in reactions producing potential etchant species? This and other pertinent questions can be answered by a detailed analysis of the plasma chemistry and the species transport and reaction in the plasma reactor.

Figure 1 shows partial energy level diagrams for argon and chlorine. The argon metastable species ($^3P_2$ and $^3P_0$) have a relatively high energy and also a long lifetime because their transition to the ground state is forbidden. Consequently, metastables can participate actively in the plasma chemistry. For example, metastables have been found to play an important role in the pristine argon discharge in both dc[4] and rf[5] systems despite the fact that their mole fraction is $\sim 10^{-5}$. The metastable levels interact strongly with the resonant levels ($^3P_1$ and $^1P_1$), as well as a set of higher lying levels (shown as one level in Fig. 1). The higher lying levels actually redistribute the metastable and resonant (M&R) species[6] since they are produced by electron impact excitation of M&R and they are lost by radiative decay back to the M&R levels (collisional-radiative mixing). When Cl_2 is added to Ar, metastables can induce dissociation or ionization of chlorine (Penning effect).

In this work, a plasma chemistry model was developed for a pure Ar discharge and Ar/Cl_2 mixtures. By changing the composition of the mixture, one can cover the whole range from strongly electronegative (100% Cl_2) to strongly electropositive (100% Ar) discharges. Electron transport and reaction coefficients were calculated through solution of the spatially homogeneous Boltzmann equation. The effect of species produced in the plasma (metastables, resonants, atomic chlorine) was taken into account self-consistently. A set of balance equations was solved simultaneously to provide the density of plasma species and the self-sustaining electric field (hence electron energy). This article presents a comparison between a pure Ar plasma and one with 95% Ar–5% Cl_2 (hereafter to be referred to as *the mixture*).

II. MATHEMATICAL MODEL

Large scale time-dependent multidimensional simulations of plasma reactors provide a detailed description of the spatiotemporal variation of species density, energy, and flux, as well as the self-consistent electric field distribution.[7] However, these simulations are computationally very time consuming, especially when mixed-gas plasmas are considered in which there is a plethora of species and chemical reactions. The purpose of the present model is to provide a computationally efficient means of calculating the properties of mixed gas-plasmas as the composition of the mixture varies. The details of the discharge are not sought and only space-averaged quantities are of interest here. Hence a "well mixed" reactor is assumed. Simplified models such as this can be used for a rapid evaluation of expected reactor performance as different gases are added to the plasma. The model is only limited by the availability of electron impact cross sections and information on reactions among charged and neutral species.

The goal is to predict the important species densities (electrons, ions, metastables, resonant states, atomic chlorine) and electron energy as a function of externally controllable variables such as feed gas composition, pressure, power, gas flow rate, etc. To meet this goal, a two-step approach is used. First, the Boltzmann transport equation is solved to calculate the electron energy distribution function (EEDF) and in turn the transport and reaction rate coefficients of the electron gas. These quantities are then used in species density and electron energy balance equations to obtain the self-sustaining electric field and the plasma gas composition. The reactions considered and their rate coefficients are shown in Table I. The steady-

a)Author to whom correspondence should be addressed.

 0021-8979/94/75(4)/1931/9/$6.00

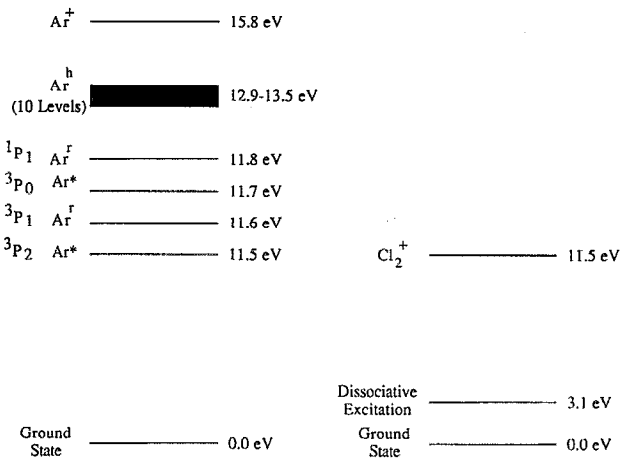

FIG. 1. Partial energy level diagrams of argon and molecular chlorine.

state model is applicable to the positive column of a dc discharge. However, the model may also be used to provide guidelines for high frequency discharges. A similar method of approach as used in the present work has been utilized before to model excimer lasers,[8–11] albeit the conditions are very different from ours (10–1000 s of Torr vs 1 Torr, and $10–10^5$ s of W/cm^3 vs 0.1 W/cm^3). This diversity shows that this method of approach is quite flexible and can be applied over a wide range of conditions.

A. Electron transport and reaction coefficients

The electron transport (diffusivity, drift velocity) and reaction (ionization, dissociation, excitation, etc.) coefficients were obtained by solving the spatially homogeneous Boltzmann equation

TABLE I. Reactions and rate coefficients in argon and argon/chlorine plasmas.

Description	Reaction	Coefficient	Value (cm^3/s)	Reference
Excitation to argon metastables	$Ar+e^-\rightarrow Ar^*+e^-$	k_e	a	23
Excitation to argon resonants	$Ar+e^-\rightarrow Ar^r+e^-$	k_{er}	a	24
Metastable argon ionization	$Ar^*+e^-\rightarrow Ar^+ +2e^-$	k_{im}	a	25
Resonant argon ionization	$Ar^r+e^-\rightarrow Ar^+ +2e^-$	k_{ir}	a	25
Ground state argon ionization	$Ar+e^-\rightarrow Ar^+ +2e^-$	k_i	a	26
Two-metastable argon ionization	$Ar^*+Ar^*\rightarrow Ar^+ +Ar+e^-$	k_{mm}	1.2×10^{-9}	6
Metastable-resonant argon ionization	$Ar^*+Ar^r\rightarrow Ar^+ +Ar+e^-$	k_{rm}	2.1×10^{-9}	6
Metastable quenching to resonant	$Ar^*+e^-\rightarrow Ar^r+e^-$	k_r	2.0×10^{-7}	4
Metastable quenching to higher states	$Ar^*+e^-\rightarrow Ar^h+e^-$	k_{mh}	b	27
Two-body quenching of argon metastables	$Ar^*+Ar\rightarrow 2Ar$	k_{2q}	2.1×10^{-15}	28
Three-body quenching of argon metastables	$Ar^*+2Ar\rightarrow 3Ar$	k_{3q}	1.1×10^{-32}	29,c
Metastable superelastic collisions	$Ar^*+e^-\rightarrow Ar+e^-$	k_{se}	a	
Resonant quenching to higher states	$Ar^r+e^-\rightarrow Ar^h+e^-$	k_{rh}	b	27
Resonant superelastic to metastables	$Ar^r+e^-\rightarrow Ar^*+e^-$	k_{rs}	3.0×10^{-7}	4,29
Three-body quenching of argon resonants	$Ar^r+2Ar\rightarrow 3Ar$	k_{r3q}	1.2×10^{-32}	6,c
Resonant superelastic collisions	$Ar^r+e^-\rightarrow Ar+e^-$	k_{rse}	a	
Radiative decay of resonants	$Ar^r\rightarrow Ar+h\nu$	$1/\tau$	1.0×10^5	30,d
Radiative decay of higher states	$Ar^h\rightarrow Ar^*+h\nu$	δ_{hm}		27
	$\rightarrow Ar^r+h\nu$	δ_{hr}		27
Chlorine quenching of metastables	$Ar^*+Cl_2\rightarrow ArCl^*+Cl$	k_{qCl_2}	71×10^{-11}	17
	$\rightarrow Ar+2Cl$			
	$\rightarrow Ar+Cl_2^*$			
	$\rightarrow Ar+Cl_2^+ +e^-$			
Chlorine quenching of resonants	$Ar^r+Cl_2\rightarrow ArCl^*+Cl$	k_{qCl_2}	71×10^{-11}	17
	$\rightarrow Ar+2Cl$			
	$\rightarrow Ar+Cl_2^*$			
	$\rightarrow Ar+Cl_2^+ +e^-$			
Molecular chlorine ionization	$Cl_2+e^-\rightarrow Cl_2^+ +2e^-$	k_{iCl_2}	a	31,32
Atomic chlorine ionization	$Cl+e^-\rightarrow Cl^+ +2e^-$	k_{iCl}	a	31,32
Dissociative attachment of chlorine	$Cl_2+e^-\rightarrow Cl^- +Cl$	k_{att}	a	31,32
Dissociation of chlorine	$Cl_2+e^-\rightarrow 2Cl+e^-$	k_{dCl_2}	a	31,32
Wall recombination of atomic chlorine	$Cl+Cl+wall\rightarrow Cl_2+wall$	γ	7×10^{-3}	e
Positive–negative ion recombination	$Cl^- +X^+\rightarrow X+Cl$	k_{rec}	5.0×10^{-8}	33,34
Volume recombination of atomic chlorine	$2Cl+M\rightarrow Cl_2+M$	k_{vr}	1.14×10^{-32}	35,c
Momentum transfer for argon	$Ar+e^-\rightarrow Ar+e^-$	k_{momA}	a	36,37
Momentum transfer for molecular chlorine	$Cl_2+e^-\rightarrow Cl_2+e^-$	k_{momCl_2}	a	33,34
Momentum transfer for atomic chlorine	$Cl+e^-\rightarrow Cl+e^-$	k_{momCl}	a	33,34

[a]Rate coefficient calculated from EEDF.
[b]W. L. Wiese and G. A. Martin, *CRC Handbook of Chemistry and Physics*, 71st ed. (CRC, Boca Raton, FL, 1990), pp. 10-130 to 10-132.
[c]Units are cm^6/s.
[d]Units are s^{-1}.
[e]Dimensionless.

$$\frac{\partial f}{\partial t}-\frac{eE}{m}\nabla_v f=\left(\frac{\delta f}{\delta t}\right)_{\text{col}}, \tag{1}$$

where f is the electron velocity distribution function (EVDF), e is the electron charge, E is the electric field, and m is the electron mass. The term on the right hand side of the equation is the collision integral which accounts for electron energy transferred in elastic and inelastic collisions. The collisions included in this work and the sources for their cross sections are shown in Table I. For a nearly isotropic distribution with a small perturbation due to an electric field the two-term expansion can be applied[12,13]

$$f\approx f_0+\frac{\mathbf{v}}{v}\cdot\mathbf{f}_1. \tag{2}$$

In a dc discharge the EVDF depends on the electric field to neutral density ratio E/N and the plasma gas composition. In this work the effect on the EVDF of excited species and radicals produced by excitation and dissociation of the feedstock gas was included in a self-consistent manner. Electron–electron collisions were found to be unimportant for the conditions examined.

Knowing the distribution function, the electron transport and reaction coefficients can be found. The rate coefficients are determined using[14,15]

$$k_j=\left(\frac{2e}{m}\right)^{1/2}\int_0^\infty \sigma_j(\varepsilon)\varepsilon f_0(\varepsilon)d\varepsilon, \tag{3}$$

where σ_j is the cross section for the jth reaction, ε is the electron energy, and $f_0(\varepsilon)$ is the isotropic part of the distribution function expressed in terms of energy, i.e., the electron energy distribution function (EEDF). The drift velocity is given by

$$v_d=-\frac{1}{3}\left(\frac{E}{N}\right)\left(\frac{2e}{m}\right)^{1/2}\left[\int_0^\infty \frac{1}{[\Sigma_s\delta_s\sigma_s(\varepsilon)]}\frac{df_0}{d\varepsilon}\varepsilon\, d\varepsilon\right]=\mu_e E, \tag{4}$$

where s is the number of species, $\delta_s=N_s/N$ is the mole fraction of species s, and μ_e is the electron mobility.

In practice, the Boltzmann equation was solved for a set of values of E/N and mole fraction of the species of interest. Look up tables were used to interpolate for the electron transport and reaction coefficients needed for the balance equations described below.

B. Plasma model

1. Electron density balance

The electron density balance is written as

$$k_{\text{im}}N_{\text{Ar}*}N_e+k_{\text{ir}}N_{\text{Ar}^r}N_e+k_{\text{i}}N_{\text{Ar}}N_e+\tfrac{1}{2}k_{\text{mm}}N_{\text{Ar}*}^2+k_{\text{rm}}N_{\text{Ar}*}N_{\text{Ar}^r}+k_{\text{iCl}_2}N_{\text{Cl}_2}N_e+k_{\text{iCl}}N_{\text{Cl}}N_e-k_{\text{att}}N_{\text{Cl}_2}N_e-\frac{D_a N_e}{\Lambda^2}=0, \tag{5}$$

where k_{im}, k_{ir}, k_{i}, k_{mm}, k_{rm}, k_{iCl_2}, k_{iCl}, and k_{att}, represent rate coefficients for metastable ionization, resonant ionization, ground state argon ionization, metastable-metastable (pooling) ionization, resonant-metastable ionization, molecular chlorine ionization, atomic chlorine ionization, and attachment to molecular chlorine, respectively. Also, N_{Ar}, $N_{\text{Ar}*}$, N_{Ar^r}, N_{Cl_2}, N_{Cl}, and N_e are the density of ground state argon, metastable argon, resonant argon, molecular chlorine, atomic chlorine, and electrons, respectively. D_a is the ambipolar diffusion coefficient and Λ is the characteristic diffusion length (0.78 cm in this case, corresponding to our experimental reactor). The ambipolar diffusion coefficient for a mixture of electrons, positive ions, and negative ions has been calculated by Rogoff.[16] In the case of pure argon, the terms containing N_{Cl_2} and N_{Cl} in Eq. (5) were set equal to zero. Ar^+–electron recombination and dissociative recombination of Cl_2^+ with electrons were found to be negligible for pressures less than 1 Torr examined in this article. In addition, the Ar_2^+ density was estimated based on production of molecular ions by three-body collisions with neutrals and loss by dissociative recombination and ambipolar diffusion. The molecular ion density was found to be less than 2% of the positive ion density for pressures <1 Torr. Based on this finding, electron loss by dissociative recombination with the dimer ions is negligible.

2. Metastable argon balance

To simplify the analysis, the two metastable levels are lumped into one state (the $^3P_2$ level has much higher density than the $^3P_0$ level anyway[4]). The metastable argon balance is written as

$$k_e N_e N_{\text{Ar}}+k_{\text{rs}}N_{\text{Ar}^r}N_e+\left(\sum_h k_{\text{rh}}\delta_{\text{hm}}\right)N_e N_{\text{Ar}^r}-N_{\text{Ar}*}\left[k_{\text{im}}N_e+k_{\text{mm}}N_{\text{Ar}*}+k_{\text{rm}}N_{\text{Ar}^r}+k_r N_e+k_{\text{se}}N_e+k_{2\text{q}}N_{\text{Ar}}+k_{3\text{q}}N_{\text{Ar}}^2+\left(\sum_h k_{\text{mh}}\delta_{\text{hr}}\right)N_e+\frac{D_m}{\Lambda^2}\right]-k_{q\text{Cl}_2}N_{\text{Cl}_2}N_{\text{Ar}*}=0. \tag{6}$$

The first three terms represent production of metastables via ground state excitation, direct conversion of the resonant to the metastable state by electron collisions, and indirect conversion of the resonant to the metastable state by way of the higher lying $4p$ states, respectively. The loss terms for pure argon (long term in brackets) are metastable (two-step) ionization, metastable-metastable ionization, resonant-metastable ionization, electron quenching to the resonant state, superelastic collisions to ground state, two-body quenching, three-body quenching, transitions to the resonant state by way of the higher lying states, and diffusion to the walls of the container. The final metastable loss term is quenching of metastables by molecular chlorine which is nonzero only for the argon chlorine mixture. Quenching by atomic chlorine is not expected to be nearly as effective as that by molecular chlorine and it is neglected.

The term

$$\left(\sum_h k_{rh}\delta_{hm}\right)N_eN_{Ar^r}$$

and also the term

$$\left(\sum_h k_{mh}\delta_{hr}\right)N_eN_{Ar*}$$

in Eq. (9) represents the redistribution of metastable and resonant species by transitions with higher lying states. The branching ratios in these terms are calculated in the following manner:[4]

$$\delta_{hj}=\frac{A_{hj}}{(\Sigma_{j=1}^{4}A_{hj})}, \tag{7}$$

where δ_{hj} is the branching ratio, h is a particular higher lying level, j is a metastable or resonant level, and A_{hj} is the atomic transition probability for the h to j transition. Similarly, the rate coefficients k_{jh} are calculated by

$$k_{jh}=\bar{k}\frac{f_{jh}}{(\Sigma_{h=1}^{10}f_{jh})}, \tag{8}$$

where $\bar{k}$ is the mean rate coefficient (2.0×10^{-6} cm^3/s) (Ref. 4), and f_{jh} is the experimental line strength for the j to h transition.

3. Resonant argon balance

As for the metastables, the two resonant levels are lumped into one state. The resonant argon balance is similar to the metastable balance and can be written as

$$k_rN_eN_{Ar*}+k_{er}N_eN_{Ar}+\left(\sum_h k_{mh}\delta_{hr}\right)N_eN_{Ar*}$$
$$-N_{Ar^r}\left[\frac{1}{\tau}+k_{rs}N_e+k_{r3q}N_{Ar}^2+k_{ir}N_e+k_{mr}N_{Ar*}+k_{r2q}N_{Ar}\right.$$
$$\left.+k_{rsc}N_e+\left(\sum_h k_{rh}\delta_{hm}\right)N_e\right]-k_{qCl_2}N_{Ar^r}N_{Cl_2}=0. \tag{9}$$

In order of appearance in Eq. (9), the terms from left to right represent resonant generation by electron impact quenching of metastables, by ground state excitation, and from metastables via the higher lying states. Resonants are lost by radiation, superelastic collisions to metastables, three-body quenching, resonant ionization, metastable-resonant ionization, superelastic collisions to ground state, transitions to metastables via higher lying states, and, in the presence of chlorine, quenching by molecular chlorine.

4. Negative chlorine ion balance

In the case of the argon/chlorine mixture, a balance was written on the negative chlorine ions as follows:

$$k_{att}N_{Cl_2}N_e=k_{rec}N_{Cl^-}N_+. \tag{10}$$

Negative ions are formed by dissociative attachment to molecular chlorine, and are lost by recombination with positive ions. In Eq. (10) it is assumed that negative ions recombine with the three different kinds of positive ions (Ar^+, Cl_2^+, and Cl^+) with the same rate coefficient k_{rec}. Equation (10) is combined with the total charge balance

$$N_{Cl^-}+N_e=N_+ \tag{11}$$

to give the negative ion density.

Separate positive ion density balances were not included in the model. Instead, the positive ions were lumped and their density was obtained from the electroneutrality constraint [Eq. (11)]. In our model, the ion composition will affect the ambipolar diffusion loss of electrons. To assess the effect of uncertainty in the ambipolar diffusivity D_a, calculations were done by changing the positive ion mobility μ_+ by 50% upwards and downwards, an extreme variation. Results on electron density changed by less than 10% while the metastable and Cl-atom density change was even smaller. Hence the precise ion composition is not important in determining the electron, metastable, and Cl-atom densities for the high pressure–low electron density plasma system examined in this article.

In separate calculations under low pressure–high plasma density (10 mTorr, 10^{11}–10^{12}/cm^3) conditions, we found that the precise ion composition must be known in order to obtain the correct electron and Cl-atom density. However, those conditions are outside the scope of the present article.

5. Atomic chlorine balance

A balance was written on atomic chlorine to predict the degree of dissociation of molecular chlorine in the argon/chlorine mixture. This balance is

$$k_{att}N_{Cl_2}N_e+2k_{dCl_2}N_{Cl_2}N_e+k_{rec}N_+N_{Cl^-}+fk_{qCl_2}N_{Cl_2}N_{Ar*}$$
$$-k_{iCl}N_{Cl}N_e-k_{vr}N_{Cl}^2N-\frac{QN_{Cl}}{V}-\frac{N_{Cl}v_{Cl}\gamma}{4}\left(\frac{S}{V}\right)=0. \tag{12}$$

In this equation, k_d and k_{vr} are rate coefficients for dissociative excitation of molecular chlorine and volume recombination of atomic chlorine, respectively. Q, V, S, v_{Cl}, and γ are gas flow rate (at reactor conditions), plasma volume, surface area available for atom recombination, thermal speed, and wall recombination probability of chlorine atoms, respectively. The first four terms represent the production of atomic chlorine by dissociative attachment, dissociation, ion–ion recombination, and quenching of metastable argon, respectively. The branching ratio of the metastable quenching reaction to atomic chlorine is denoted by $f=0.66$.[17] The last four terms represent loss of atomic chlorine by ionization, volume recombination, flow out of the reactor, and wall recombination. To determine the density of molecular chlorine, which is needed as an input to this equation, a total chlorine species balance is performed. This balance is

$$N_{Cl_2}=0.05N-0.525N_{Cl} \tag{13}$$

and is derived from the fact that at the reactor inlet, there is 5% molecular chlorine in 95% argon. N is the total gas density

6. Power density balance

The power density balance used here

$$\bar{P}=eN_e\mu_eE^2 \tag{14}$$

is the same one used by Karoulina and Lebedev,[6] where $\bar{P}$ is power per unit plasma volume. The electron density in the mixture is an order of magnitude lower than the negative (and positive) ion density. However, the ionic mobility is three orders of magnitude lower than the electron mobility. Hence the power transferred to the ions may be neglected. Because $v_d=\mu_eE$, the power density balance may also be written as

$$\bar{P}=eN_ev_d\frac{E}{N}N. \tag{15}$$

This is the form of the equation used in the model. The drift velocity needed for this equation was calculated through the EEDF. Equation (15) does not account for any power dissipation in the sheath, since the model is written for a bulk plasma. Simple extensions of this model can include terms to account for power losses in the sheath region.

III. METHOD OF SOLUTION

The electron transport and reaction coefficients in Eqs. (5), (6), (9), (10), (12), and (15) depend implicitly on E/N, which is one of the unknowns. The equations are further coupled through the species densities. The system of equations was solved using a continuation algorithm DERPAR[18] to find E/N, N_{Ar^*}, N_{Ar^r}, N_{Cl}, N_{Cl_2}, N_{Cl^-}, and N_e as a function of pressure for input values of power density. It is necessary to have a good initial guess of the solution at some point in the pressure range considered (0.3 to 1.0 Torr). Good initial estimates for the solution keep the errors low as calculations are made further away from the initial point. In all cases, the balance equations achieved closure to within less than 0.1%.

IV. RESULTS

A. Boltzmann transport model

The EEDF calculated for pure argon is compared to the one for a mixture of 5% Cl_2 in argon (at the same E/N) in Fig. 2. The EEDFs are normalized such that

$$\int_0^\infty \varepsilon^{1/2}f_0(\varepsilon)d\varepsilon=1. \tag{16}$$

The EEDF for pure argon has a longer tail than that for the mixture. Chlorine has several vibration and excitation levels with threshold energies well under 10 eV (the lowest excitation level for argon is at 11.5 eV). These processes are a substantial sink of electron energy resulting in depletion of the the tail of the EEDF, even when only a small amount of chlorine is added to argon.

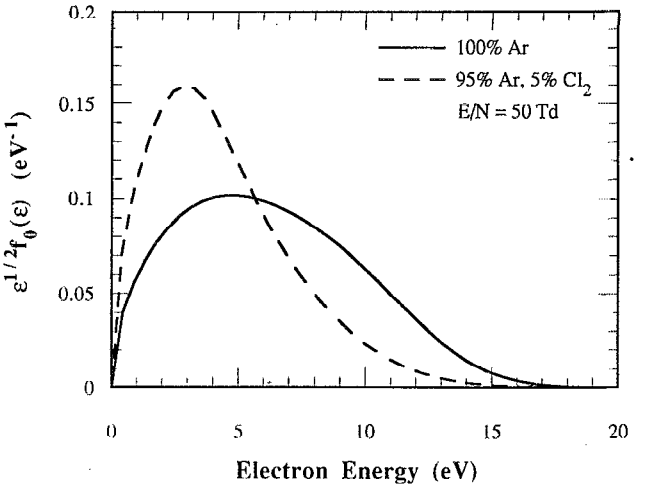

FIG. 2. Electron energy distribution function for pure argon and 95% Ar/5% Cl_2 mixture.

The differences in the EEDFs for pure argon and the argon/chlorine mixture manifest themselves in the calculated electron-impact reaction coefficients as shown in Table II. For high threshold energy transitions (greater than 10 eV, such as excitation to the metastable or resonant state of argon, or ground state argon ionization), the rate coefficients differ by an order of magnitude. For lower threshold energy transitions, such as metastable or resonant argon ionization, the rate coefficients only differ by a factor of 2. These results demonstrate the sensitivity of the electron-impact reaction rate coefficients to even a few % addition of a molecular gas to argon. Similar results are expected by adding other gases with relatively low threshold processes (vibration, dissociation) to argon or to other noble gases.

Figure 3 shows the EEDFs for pure argon in more detail. The tail of the EEDF changes significantly by including a small fraction of metastables. The tail is extended to higher energies, apparently by the effect of superelastic collisions with metastables which feed energy back to the electrons. The effect is absent when the metastable density is set to zero, and becomes more pronounced as the metastable mole fraction increases. Modification of the tail of the EEDF can have profound effect on high threshold energy processes. However, the mean electron energy which is dominated by the low energy electrons remains essen-

TABLE II. Rate coefficient comparison (E/N=50 Td).

	Pure argon	95% argon/5% chlorine
k_e (cm^3/s)	1.14×10^{-10}	2.02×10^{-11}
k_{er} (cm^3/s)	7.67×10^{-11}	1.33×10^{-11}
k_i (cm^3/s)	1.39×10^{-11}	1.57×10^{-12}
k_{ve} (cm^3/s)	1.66×10^{-9}	6.41×10^{-10}
k_{rs} (cm^3/s)	1.05×10^{-9}	8.36×10^{-10}
k_{im} (cm^3/s)	6.68×10^{-8}	3.31×10^{-8}
k_{ir} (cm^3/s)	6.68×10^{-8}	3.31×10^{-8}
k_{mom} (cm^3/s)	1.26×10^{-7}	9.10×10^{-8}

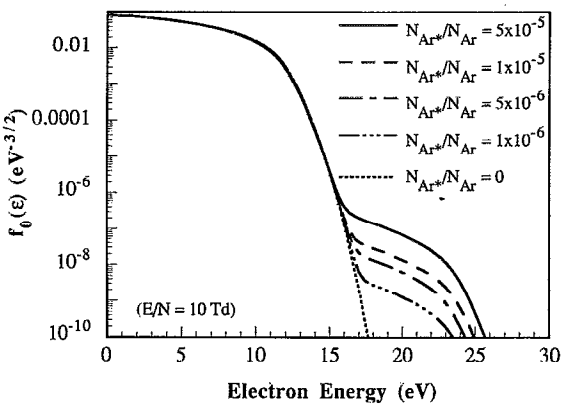

FIG. 3. Effect of metastable argon density on the electron energy distribution function for pure argon.

tially unaffected. Figure 3 also shows that the EEDFs are non-Maxwellian (a Maxwellian EEDF would be a straight line on this plot). For pure argon, a two-temperature model appears to be applicable.

B. Plasma model

The calculated self-sustaining E/N for a pristine argon discharge and for a 5% Cl_2 mixture in argon are shown in Fig. 4. In the pressure range between 0.3 and 1.0 Torr which corresponds to $N\Lambda$ of 7.5×10^{15} to 2.5×10^{16} cm^{-2} (for a gas temperature of 300 K and a characteristic diffusion length $\Lambda=0.78$ cm). E/N varies between 32.4 and 11.2 Td for pure argon and between 129.4 and 80.3 Td for the mixture. For low $N\Lambda$, E/N is high because ambipolar diffusion of electrons to the walls becomes more important, and it is necessary to have higher E/N to increase the ionization rate and counter the diffusive losses of electrons. The sustaining E/N is much higher for the mixture compared to pure argon. As chlorine is added to argon, the tail of the EEDF is reduced (see Fig. 2) and high threshold processes, in particular ionization, happen at a much reduced rate. Furthermore, attachment to molecular chlorine adds to electron losses. Hence the self-sustaining E/N has to increase as one adds chlorine to argon in order to satisfy the electron density balance [Eq. (5)].

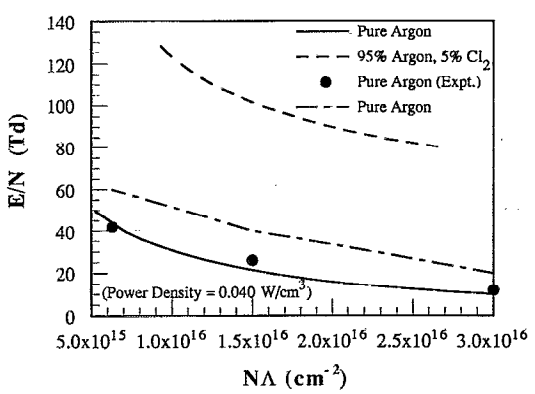

FIG. 4. Calculated E/N for pure argon (solid line) and 95% Ar/5% Cl_2 mixture (dashed line). Experimental data (●) and model predictions (chain line) for pure argon are from Ferreira *et al.* (Ref. 4).

TABLE III. Electron production mechanisms ($N\Lambda=2.5\times10^{16}$ cm^{-2}, 0.040 W/cm^3).

Process	Pure argon	95% argon/ 5% chlorine
Ground state argon ionization	0.8	44.8
Metastable argon ionization	56.1	0.0
Resonant argon ionization	28.2	0.0
Two-metastable argon ionization	5.4	0.0
Metastable-resonant argon ionization	9.5	0.0
Molecular chlorine ionization	0.0	35.9
Atomic chlorine ionization	0.0	19.3

Theoretical results of Ferreira *et al.*[4] as well as their experimental data for pure argon are also shown in Fig. 4. Our calculations are in satisfactory agreement with the experimental data. Ferreira and Ricard[19] also predicted E/N for pure argon theoretically, but their values were a factor of 3 too high. Although they included a metastable density balance in their model, they did not include the effect of metastables in calculating the electron-impact rate coefficients. They claimed that their calculated values would be closer to the experimental data if they included this effect. In Ref. 4, they did include the effect of metastables on the rate coefficients, but their calculated E/N (as shown in Fig. 4 of the present work) is still too high compared to their experimental values. McCaughy and Kushner[20] calculated an E/N of 15 Td in a dusty argon plasma, for a low dust density. They included metastables and metastable ionization in their calculations, and their results compare closely with those of Ferreira and coworkers and the present results. The above discussion underlines the importance of including the argon metastable species in a self-consistent manner in order to accurately model the plasma. This conclusion was also reached in connection with a radio frequency argon discharge.[5] Unfortunately, we could not locate any experimental data on E/N for a 5% mixture of Cl_2 in argon to compare against our calculations.

Table III shows the percentage for electron production and loss processes for pure argon and the mixture at the corresponding self-sustaining E/N for an $N\Lambda$ value of 2.5×10^{16} cm^{-2}. For the pure argon case ($E/N=12$ Td), electron production comes primarily from the two-step ionization of metastable and resonant species. However, when Cl_2 is added to argon, metastables and resonant states are quenched, and the operating E/N increases to 80 Td. Then ionization of ground state argon becomes dominant with molecular and atomic chlorine ionization following in order of importance.

Figure 5 shows E/N as a function of $N\Lambda$ for the mixture and for varying power density. As power density increases, E/N decreases for the mixture. This is in part because of reduced electrons losses by attachment as more molecular chlorine is dissociated by increasing power density. In contrast, increasing the power density from 0.004

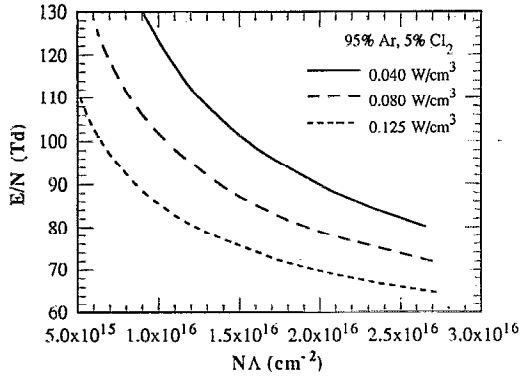

FIG. 5. Effect of power on E/N for 95% Ar/5% Cl_2 mixture.

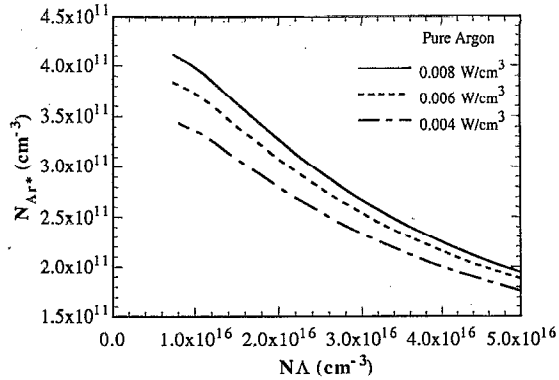

FIG. 7. Effect of power on the metastable argon density in pure argon.

to 0.008 W/cm^3 had only a minor effect on the E/N for pure argon.

The calculated argon metastable density as a function of $N\Lambda$ is shown in Fig. 6. As the pressure, and thus $N\Lambda$, is decreased, the metastable density increases. The same trend was observed for the argon resonant states, although the density of the resonants was several times lower. As $N\Lambda$ decreases, the operating E/N increases and the production of metastables by excitation of ground state argon also increases. On the other hand, metastable losses (quenching to resonant and higher states) are not as sensitive to changes of E/N because they are lower energy processes. Table IV shows that for an $N\Lambda$ value of 2.5×10^{16} cm^{-2}, 53.5% of metastables in pure argon and 99.8% of metastables in the mixture are produced by excitation of ground state argon atoms. Furthermore, Table IV helps illustrate why the metastable density is an order of magnitude higher in the pure argon compared to the mixture. For pure argon, the primary quenching mechanism is collisions with electrons, while for the mixture it is collisions with Cl_2. The chlorine quenching reaction has a large rate coefficient (Table I). Thus, even a few % of Cl_2 addition to pure argon decreases the metastable density by an order of magnitude. Figure 6 also shows that, in the mixture, the metastable density increases with power density. Increased molecular dissociation with power density, and hence reduced quenching of metastables, is responsible for this effect. In contrast, power density does not have much influence on metastable density in the pure argon discharge (Fig. 7), over the limited power density range examined.

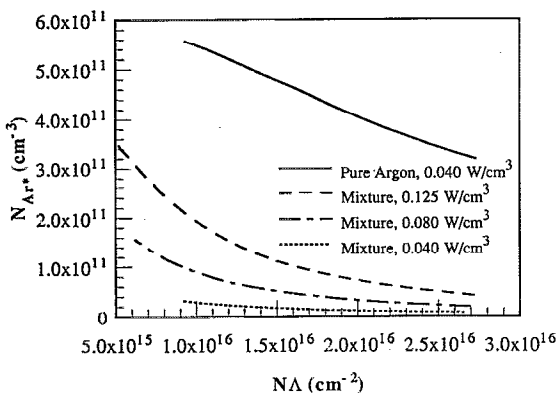

FIG. 6. Metastable argon density for pure argon and 95% Ar/5% Cl_2 mixture.

Argon metastable densities have been measured experimentally for pure argon dc discharges by optical absorption[4,19,21] and for rf plasmas by laser induced fluorescence.[2,3] For a pressure of 0.3 Torr ($N\Lambda=8\times10^{15}$ cm^{-2}), the laser induced fluorescence measurements taken at a power density of 0.41 W/cm^3 yielded argon metastable densities of 1×10^{11} cm^{-3}. The absorption measurements, taken at 0.15 Torr and a current density of 0.0038 A/cm^2, yielded metastable densities of 2×10^{11} cm^{-3} for the $^3P_2$ state and 2.5×10^{10} cm^{-3} for the $^3P_0$ state. The metastable densities calculated with the present model are comparable to those measured in the literature. Scheller *et al.*[3] used laser-induced fluorescence (LIF) to measure the relative density of argon metastables in an rf argon discharge while adding small amounts of chlorine. As they increased the mole fraction of Cl_2 to 5%, they observed a drop in the LIF intensity by an order of magnitude. This result is similar to that shown in Fig. 6.

The electron density is much higher for pure argon than for the mixture due to the strong attachment to molecular chlorine in the mixture (Fig. 8). Attachment is also responsible for the creation of negative ions, which are the dominant negative species in the mixture. It is worth noting that the dependence of electron density on pressure (or $N\Lambda$) is different in pure argon compared to the mixture. For the pure argon case, the electron density increases with increasing pressure. This is due to reduced ambipolar diffusion losses and increased number density of molecules available for ionization as pressure increases. This trend was also seen by Ohwa, Moratz, and Kushner[22] in an Ar/Xe mixture at higher pressures. However, when chlorine is added, attachment becomes important at higher pressures, and this offsets the inverse proportionality of the ambipolar diffusion on pressure.

Figure 9 shows the atomic chlorine density as a function of $N\Lambda$ for three power densities for the argon/chlorine mixture. The atomic chlorine density decreases with de-

TABLE IV. Metastable argon production and loss mechanisms ($N\Lambda=2.5\times10^{16}$ cm^{-2}, 0.040 W/cm^3).

Process	Metastable argon production (%)	
	Pure argon	95% argon/5% chlorine
Ground state excitation	53.5	99.8
Resonant superelastic collisions	9.6	0.0
Quenching from higher states	36.9	0.2
	Metastable argon loss (%)	
Quenching to resonant state	12.7	0.0
Metastable ionization	3.2	0.0
Two-metastable ionization	0.6	0.0
Metastable-resonant ionization	0.5	0.0
Two- and three-body quenching	0.1	0.0
Superelastic collisions	0.1	0.0
Quenching to higher states	82.5	0.3
Diffusion	0.2	0.0
Chlorine quenching	0.0	99.6

creasing pressure and/or power. However, the mole fraction of atomic chlorine in the mixture increases from 3.7% at $N\Lambda=2.5\times10^{16}$ cm^{-2} to 4.7% at an $N\Lambda=1\times10^{16}$ cm^{-2} (i.e., the mole fraction increases with decreasing pressure) for a power density of 0.040 W/cm^3.

V. SUMMARY AND CONCLUSIONS

A steady-state model has been developed to predict how the important species density and electron energy change when an electronegative gas is added to a noble gas discharge. The Boltzmann transport equation was solved to obtain the electron transport and reaction coefficients as a function of plasma gas composition. Thus, the effect of excited (metastable, resonant) and radical species generated in the plasma was taken into account in a self-consistent manner. The same methodology can be used to model other plasma systems as well. The model may also be useful for estimating important species densities in the bulk plasma of high frequency mixed-gas discharges.

The model was used to compare a pure argon discharge to a 5% Cl_2/95% Ar mixture. For a given E/N, the EEDF for the mixture showed a much shorter tail. This resulted in much lower rate coefficients for the high threshold energy electron-impact reactions. Specifically, excitation and ionization rate coefficients can be an order of magnitude lower in the mixture.

The self-sustaining E/N for the mixture was much higher than for pure argon. This is due to the lower rate coefficients for ionization (see previous paragraph) and also because of electron attachment in the mixture. The predicted E/N for a pure argon discharge was in good agreement with available experimental data. The predicted argon metastable density decreased by an order of magnitude by the addition of only 5% chlorine to an argon plasma due to efficient quenching of metastables by molecular chlorine. Scheller *et al.*[3] observed a similar reduction in metastable density in an rf plasma reactor. The predicted argon metastable density compared favorably to those found in the literature for the pure argon case as well. Power density has a small effect on the pure argon plasma,

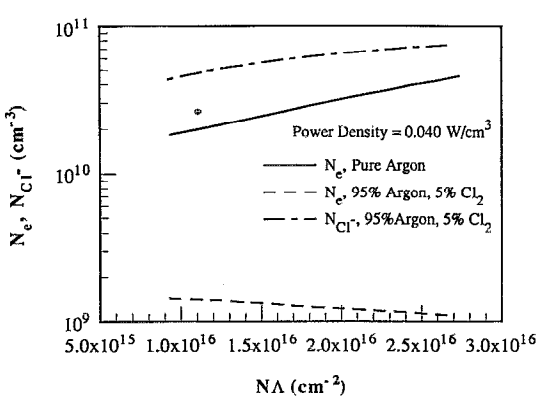

FIG. 8. Electron and negative ion densities in pure argon and 95% Ar/5% Cl_2 mixture.

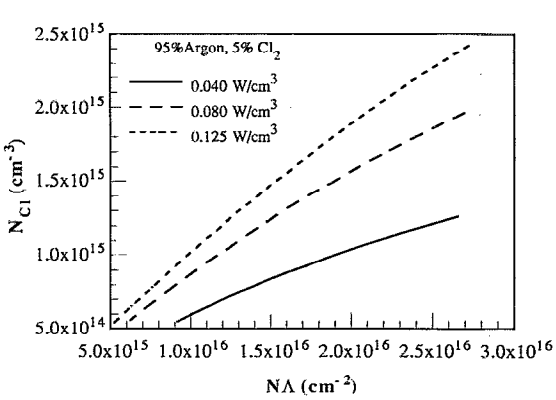

FIG. 9. Effect of power on atomic chlorine densities in 95% Ar/5% Cl_2 mixture.

but a pronounced effect on the argon/chlorine mixture. In general, the metastable, resonant, and atomic chlorine densities increase with increasing power density, but the self-sustaining E/N decreases with increasing power density.

The model presented here may be used as a template to predict the effect of additives in noble and reactive gas plasmas. The only limitation is availability of electron-impact cross sections and reaction rate coefficients among neutral and charged species. Results for other gas compositions and more detailed comparisons with experimental data will be reported elsewhere.

ACKNOWLEDGMENT

We are grateful to the Welch Foundation for financial support of this work.

[1] O. Krogh, T. Wicker, and B. Chapman, J. Vac. Sci. Technol. B **4**, 1292 (1986).
[2] R. A. Gottscho, G. R. Scheller, T. Intrator, and D. B. Graves, J. Vac. Sci. Technol. A **6**, 1393 (1988).
[3] G. R. Scheller, R. A. Gottscho, T. Intrator, and D. B. Graves, J. Appl. Phys. **64**, 598 (1988).
[4] C. M. Ferreira, J. Loureiro, and A. Ricard, J. Appl. Phys. **57**, 82 (1985).
[5] D. P. Lymberopoulos and D. J. Economou, J. Appl. Phys. **73**, 3668 (1993).
[6] E. V. Karoulina and Y. A. Lebedev, J. Phys. D **25**, 401 (1992).
[7] D. P. Lymberopoulos and D. J. Economou, Appl. Phys. Lett. **63**, 2478 (1993).
[8] W. L. Nighan, IEEE J. Quantum Electron. **QE-14**, 714 (1978).
[9] H. Kumagai and M. Obara, IEEE Trans. Plasma Sci. **16**, 453 (1988).
[10] V. Mihkelsoo, P. Miidla, V. Peet, A. Sherman, E. Tamme, and A. Treshchalov, J. Phys. B **22**, 1489 (1989).
[11] M. Ohwa and M. Obara, J. Appl. Phys. **63**, 1306 (1988).
[12] W. L. Morgan, Joint Inst. for Lab. Astrophysics, Univ. of Colorado, Boulder, Report 19, 1979.
[13] W. L. Morgan and B. M. Penetrante, Comput. Phys. Commun. **58**, 127 (1990).
[14] S. C. Brown, *Introduction to Electrical Discharges in Gases* (Wiley, New York, 1966).
[15] B. E. Cherrington, *Gaseous Electronics and Gas Lasers* (Pergamon, New York, 1979).
[16] G. L. Rogoff, J. Phys. D: **18**, 1533 (1985).
[17] L. A. Gundel, D. W. Setser, M. A. A. Clyne, J. A. Coxon, and W. Nip, J. Chem. Phys. **64**, 4390 (1976).
[18] M. Kubicek and M. Marek, *Computational Methods in Bifurcation Theory and Dissipative Structures* (Springer, New York, 1983).
[19] C. M. Ferreira and A. Ricard, J. Appl. Phys. **54**, 2261 (1983).
[20] M. J. McCaughy and M. J. Kushner, J. Appl. Phys. **69**, 6952 (1991).
[21] M. Moisan and Z. Zakrzewski, *Reactive Processes in Discharge Plasmas*, edited by J. M. Proud and L. H. Luessen (Plenum, New York, 1985).
[22] M. Ohwa, T. J. Moratz, and M. J. Kushner, J. Appl. Phys. **63**, 5131 (1989).
[23] W. L. Borst, Phys. Rev. A **9**, 1195 (1974).
[24] C. M. Ferreira and J. Loueiro, J. Phys. D **16**, 1611 (1983).
[25] E. J. McGuire, Phys. Rev. A **20**, 445 (1979).
[26] D. Rapp, and P. Englander-Golden, J. Chem. Phys. **43**, 1464 (1965).
[27] W. L. Wiese and G. A. Martin, *CRC Handbook of Chemistry and Physics*, 71st ed. (CRC, Boca Raton, FL, 1990).
[28] J. H. Kolts and D. W. Setser, J. Chem. Phys. **68**, 4848 (1978).
[29] I. Y. Baronov, V. I. Demidov, and N. B. Kolokolov, Opt. Spectrosc. **51**, 316 (1981).
[30] G. S. Hurst, E. B. Wagner, and M. G. Payne, J. Chem. Phys. **61**, 3680 (1974).
[31] G. L. Rogoff, J. M. Kramer, and R. B Piejak, IEEE Trans. Plasma Sci. **PS-14**, 103 (1986).
[32] E. S. Aydil and D. J. Economou, J. Electrochem. Soc. **139**, 1396 (1992); **139**, 1406 (1992).
[33] S. C. Deshmukh and D. J. Economou, J. Appl. Phys. **72**, 4597 (1992).
[34] M. J. Church and D. Smith, J. Phys. D **11**, 2199 (1978).
[35] A. C. Lloyd, Int. J. Chem. Kinet. **3**, 39 (1971).
[36] H. B. Milloy, R. W. Crompton, J. A. Rees, and A. G. Robertson, Aust. J. Phys. **30**, 61 (1977).
[37] L. S. Frost and A. V. Phelps, Phys. Rev. A **136**, 1538 (1964).